

A novel modified integral PES/PVB nanofiltration membrane and its application in wastewater treatment

S. Zarinabadi*

Department of Chemical Engineering, Mahshahr Branch, Islamic Azad University, Mahshahr, Iran

Received June 26, 2016; Revised September 10, 2016

This study describes the preparation Novel polyethersulfone (PES)/poly(vinylbutyral) (PVB)/titanium dioxide (TiO₂) nanoparticles integral nanofiltration membranes were prepared by dip-coating of PES membrane in PVB and TiO₂ nanoparticles aqueous solution. Glutaraldehyde (GA) was used as a cross-linker for the integral polymer membrane in order to enhance the chemical, thermal as well as mechanical stabilities. TiO₂ nanoparticles with different concentrations (0, 0.1, 0.5, 0.8 wt.%) were coated on the surface of PES/PVB integral membrane. The morphological study was investigated by atomic force microscopy (AFM), scanning surface microscopy (SEM). In addition, the membranes performances, in terms of contact angle, permeate flux, COD rejection and swelling factor were also studied. It was found that the increase in TiO₂ solution concentration can highly affect the surface morphology and filtration performance of coated membranes. The contact angle measurement and studies indicated that the TiO₂ nanoparticles successfully were coated on the surface of PES/PVB integral membranes. However, rougher surface was obtained for membranes by TiO₂ coating. The filtration performance data showed that the 0.5 wt.% TiO₂-modified membrane presents higher performance in terms of flux and COD rejection as a pollution index. Finally, TiO₂ modified membranes demonstrated the lower degree of swelling.

Keywords: nanofiltration, polyethersulfone, modification, poly (vinyl butyral) , TiO₂ nanoparticles

INTRODUCTION

With the development of global economy, the lack of water resource is becoming an increasingly crucial problem. Membrane separation such as nanofiltration (NF) technology now has been becoming an important way in the treatment and the recycling of wastewater [1, 2]. The main advantages of this process are low operating pressures, high fluxes, high rejections of multivalent salts, low investment and operation costs leading to gaining attention in many separations, and treatment processes namely water softening, waste water treatment, color removal, chemical and biological oxygen demand reduction (COD and BOD respectively), pharmaceutical and biochemical industries[3-7]. As with any other membrane process, nanofiltration is susceptible to fouling caused by adsorption of various types of foulants including: colloidal (clays, flocs) [8], organic (oils, polyelectrolytes, humics) [9, 10] and scaling (mineral precipitates) [11, 12], either in membrane pores or on membrane surfaces. Membrane fouling can cause severe flux decline and affect the quality of the water produced. Severe fouling may require intense chemical cleaning or membrane replacement. This increases the operating costs of a treatment plant and

consequently increases the overall energy consumption of separation process. So it is vital to investigate the ways and methods to develop antifouling nanofiltration membranes. In general, the fouling occurs more seriously in the hydrophobic membranes than in the hydrophilic ones because of the interactions between the solutes, microbial cells and membrane surface [13]. The preparation and characterization of nanofiltration membrane based polymer materials have aroused a great deal of interest among researchers over the past few years. PES is a commercially available, thermally stable polymer, which is used in high-performance applications due to its toughness, good thermal resistance and chemical inertness [14]. As a result, PES is one of the most important polymeric materials and is widely used in separation fields [15, 16]. Though PES and PES-based membranes have been broadly applied in separation processes, they have some disadvantages. The main disadvantage of the PES membranes is related to their relatively hydrophobic character [15]. Their hydrophobicity leads to a low membrane flux and poor anti-fouling properties, which have a great impact on PES membrane application and useful life [17]. A general method to suppress membrane fouling, especially irreversible fouling is to inhibit natural organic matter adsorption on the membrane surface by increasing hydrophilicity of the membrane surface [18]. Many investigations have revealed

* To whom all correspondence should be sent:
E-mail: szarinabadi1@yahoo.com

that increasing the membrane surface hydrophilicity can effectively reduce the membrane fouling [19]. Therefore, efforts have focused on increasing PES hydrophilicity by chemical or physical modifications such as UV irradiation [20], addition of additive [21], plasma treatment [22], and so on. Therefore there is a need to improve the hydrophobic properties of this membrane, which might be achieved by coating. One of candidate of these material which is coated to PES is poly(vinyl butyral) that is introduced in this paper.

Poly(vinyl butyral) (PVB) is a product of the reaction between poly(vinyl alcohol) (PVA) and butyl aldehyde in the presence of an acid catalyst. Its structural formula is shown as below (Fig. 1) [23].

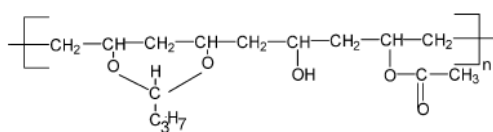


Fig. 1. Structural formula of poly(vinyl butyral).

Being an innocuous and tasteless polymeric material, PVB can endure the low temperature, light, change in humidity, bacteria, microorganism, alkali and diluent acid [24]. PVB has immense potential as membrane material because of its hydrophilicity and film forming characteristics. Swelling of PVB membrane in aqueous medium may lead to an open structure, which affects the membrane performance particularly the membrane rejection [23]. Hence there is a need to balance the hydrophilic and hydrophobic properties of such membranes. by cross-linking to PES this balance might be achieved. PVB similar to poly(vinyl alcohol) (PVA) can be cross-linked by using multifunctional compounds, such as dialdehydes [25] and dicarboxylic acids [26], which are capable of reacting with the PVB hydroxyl groups. Cross-linking improves the stability of such membranes. In this approach, glutaraldehyde (GA) was used as cross linking agent. As mentioned before, a concerning subject in membrane application is fouling. Successful utilization of membrane technology has been seriously limited by membrane fouling. A recently established method to improve the membrane antifouling properties is using TiO₂ nanoparticles on membrane structure as well as surface. TiO₂ nanoparticle has been extensively studied owing to its outstanding physical and chemical properties [27]. TiO₂ nanoparticle is usually used in the form of nanoparticles with high surface area, activity and excellent chemical stability. This nanoparticle (TiO₂) has been the

focus of numerous investigations for innocuity, resisting and decomposing bacteria, UV-proof and super hydrophilicity in recent years. Therefore, it has been applied to a variety of problems associated with water and air purification as well as environmental issues. Composite membrane with TiO₂ has better filtration performance [28] and the membrane modification with such material will introduce photocatalytic activity, which can be exploited for antifouling and regeneration purposes. In this work, the modification of PVB/PES composite nanofiltration membrane by depositing the nano-sized TiO₂ particles on the surface of PVB coated PES membranes is attempted. SEM and AFM analysis are used to examine the surface morphology of the composite nano filtration membranes. Finally as practical study, the effect of TiO₂ concentration on the COD rejection, contact angle and degree of swelling are investigated.

EXPERIMENTAL

Material

Polyethersulfone (Ultrason E6020P, MW= 58,000 g/mol) supplied from BASF company was employed as basis polymer of the membranes. TiO₂ nano powder (<40 nm), N-methyl-2-pyrrolidone (NMP) (>99.5 %), glutaraldehyde (GLU) 50% (w/w), sulfuric acid and polyvinyl pyrrolidone (PVP K 40) purchased from Merck (Germany) were used as solvent and pore former, respectively. PVB, 45–49% of butyl aldehyde group was supplied from Shanghai Chemical Reagent Company, PR China. Water used in this work was deionized beforehand.

Preparation of membranes

Polyethersulfone (PES) ultrafiltration prepared in the binary PES–solvent casting solutions by the immersion–precipitation process in which the solvent was NMP. The homogeneous solution was prepared by dissolving 16 wt.% PES in N-methyl-2-pyrrolidone (NMP) with 2 wt.% polyvinyl pyrrolidone (PVP) by stirring for 48 h at 50 °C. The polymeric solutions were subsequently coated on nonwoven-fabric, which was cut for 150mm×100mm by a stainless steel scraper at 25 °C. The scraper clearance was 200 μm (unless otherwise specified). Then, these solution films together with the nonwoven-fabric were immersed into a water bath at ambient temperature (25°C). Immediately phase inversion started, and after few minutes the resulting membranes with nonwoven-fabric separated off the stainless steel support spontaneously. The obtained membranes were then

repeatedly washed with water and wet stored. The homogeneous PVB solution which was prepared by dissolving 2 wt.% of PVB in N-methyl-2-pyrrolidone (NMP) at 50 °C for 24 h, was coated on the surface of PES barrier layer based on dip coating technique. The PVB coated membranes were then immersed in the cross-linking solution containing 5 wt.% of GA and 0.5 wt.% of H₂SO₄ for 2 min at room temperature in order to reduce the membrane swelling by chemical cross-linking. H₂SO₄ was used as catalyst of the reaction. For modification of PVB/PES composite nanofiltration membrane, TiO₂ nanoparticles with concentrations of 0.1, 0.5 and 0.8(wt.%) were dispersed in distilled water by sonication for 1 h and stirred vigorously for 45 min. Subsequently, the PVB coated membranes were immersed in TiO₂ nanoparticles solution. All modified membranes were heat treated in temperature of 110 °C for 5 min.

Scanning electron microscopy (SEM)

Structure of the prepared membranes was examined by scanning electron microscope (KYKY-EM 3200, China). For preparing the images of the cross section, the membranes were first frozen in liquid nitrogen and then fractured. After sputtering with gold, they were viewed with the microscope at 25 kV.

Atomic force microscopy (AFM)

Atomic force microscopy (AFM) was studied to analyze the surface morphology and roughness of the prepared membranes. The AFM analysis carried out by (BioScope TM, USA) using the tapping mode. All specimens with dimensions of (1cm×1cm) were cut and glued on glass substrate. The membrane surfaces were imaged in a scan size of 5 μm×5 μm.

Contact angle measurement

Membrane hydrophilicity was quantified by measuring the contact angle between the membrane surface and water. The contact angles were measured using a contact angle measuring instrument (G10, KRUSS, Germany). The contact angle values of each sample were obtained at four various positions of the sample and then the average value was recorded.

Swelling studies

The extent of membrane swelling was determined by the sorption experiments. These experiments are helpful to determine the interaction of the membranes with the liquid penetrates. The

weighed samples of circularly cut membrane pieces (3 cm diameter) have been soaked in deionized water. The membranes were weighed accurately (±0.1 mg) and kept in different soaking mixtures for 48 h. The degree of swelling (%), DS was calculated as [29]:

$$DS(\%) = \frac{M_s - M_d}{M_d} \times 100, \quad (1)$$

Where M_s and M_d are the weight of wet and dry membranes, respectively.

Nanofiltration experiments

All experiments were carried out at room temperature (25 °C) and transmembrane pressure (TMP) of 5 bar using a cross flow nanofiltration set-up with effective membrane surface area of 24 cm² in batch mode. The membranes performance was characterized by pure water flux (PWF) and yeast waste water rejection. The pure water flux was calculated by the following equation [30]:

$$J = \frac{Q}{A \times t}, \quad (2)$$

Where J is the permeation flux (L/m²h), A is the effective membrane surface area (m²) and Δt is the sampling time (h).

After pure water filtration, the feed reservoir was emptied and refilled with the feed solution in order to its filtration. The feed solutions were yeast manufacturing industry wastewater.

The solute rejection was calculated using Eq. (2) [30]:

$$R(\%) = \left(1 - \frac{C_p}{C_f}\right) \times 100\%, \quad (3)$$

Where C_p and C_f are the concentrations of the solute in permeate and feed solutions, respectively. In general, cross flow filtration system was utilized for measuring the flux and COD level of the permeate phase.

RESULTS AND DISCUSSION

AFM analysis

AFM images of the modified and unmodified membranes were shown in Fig. 2. Images recorded for PVB/PES composite membranes confirm that TiO₂ nanoparticles were successfully coated onto the membrane and produced rougher surfaces. The virgin PVB/PES membrane has smoother structure than the modified membranes with TiO₂ nanoparticles. The surface roughness parameters of membranes in scan size of 5 μm×5 μm were calculated by DME SPM software and are presented in Table 1. Ra is the mean value of surface area relative to the central plane, for which the volume enclosed by the image above and below this plane is equal. Root-mean-square (RMS) height

is a key physical parameter obtained from the AFM analysis, and defines as the mean of the root for the deviation from the standard surface to the indicated surface. The high RMS means high surface roughness. As shown in Table 1, the surface roughness of membranes modified with TiO₂ is higher than unmodified membranes.

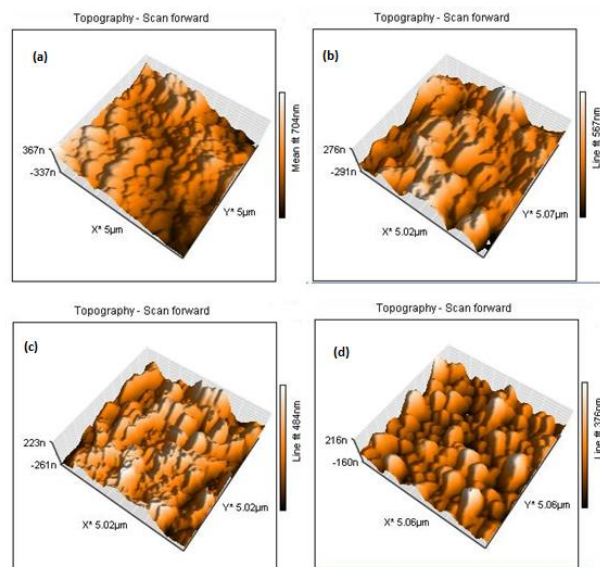


Fig. 2. AFM images of: (a) unmodified PVB/PES composite membrane, (b) 0.1 wt.% TiO₂ modified membrane, (c) 0.5 wt.% TiO₂ modified membrane, and (d) 0.8 wt.% TiO₂ modified membrane

Membrane morphology

The morphologies of unmodified PVB/PES composite membrane and PVB/PES composite modified membranes with TiO₂ nanoparticles were observed by SEM images and the obtained results are shown in Figs.3 and 4. As can be seen, in the modified PVB/PES membranes a porous top layer was formed, and a finger-like structure was observed in the sublayer of resulting membranes. The porosity of top layer is increased by increasing TiO₂ nanoparticles content. An increase with higher content of TiO₂ nanoparticles (up to 0.5 wt. %), significant agglomeration takes place. It can be seen by comparing the surface SEM images of unmodified and TiO₂nanoparticles modified membranes that there is an amount of TiO₂ nanoparticles embedding on the surface of PVB/ TiO₂ nanoparticles composite membrane. Many aggregates or chunks randomly distributed on the top surface of PVB/PES modified membranes, especially at high concentration of TiO₂

nanoparticles. Hence, the TiO₂ nanoparticles tended to form aggregates and dispersed onto the PVB/ PES membrane surface. The self-assembly of TiO₂ nanoparticles on the surface of PVB/ PES composite membrane depends on hydroxyl functional groups. The presence of hydroxyl functional groups on the surface of PVB/PES composite membrane can guarantee the self-assembly of TiO₂ and establishment of a strong bond with PVB polymer, prevents washing and removing of nanoparticles from membrane surface.

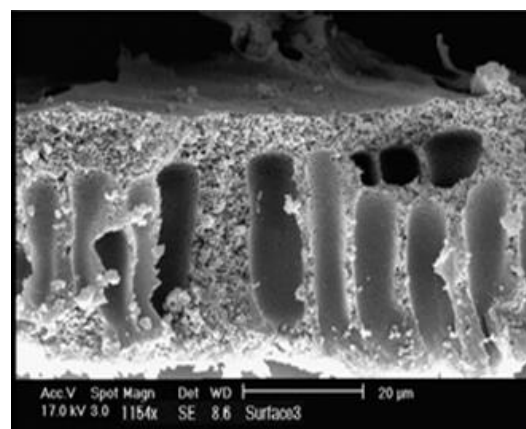


Fig. 3. The cross section SEM image of top layer of PVB/PES composite membrane.

Contact angle measurement

Fig.5 shows the effect of addition of TiO₂ nanoparticles on the contact angle and in other words wettability of the membranes. As shown, the membranes prepared with addition of TiO₂ nanoparticles present higher hydrophilicity (lower water contact angle) in comparison with the unmodified PVB/PES membrane. The highest water contact angle and in other words, the highest hydrophobicity belong to the pure PES membrane.

Coating with PVB and modified by TiO₂nanoparticles significantly improved hydrophilicity of this membrane. Water contact angle of the PVB/ PES composite membrane remarkably decreased from 71.7° to 32.3° after adding 0.5 wt. % of TiO₂nanoparticles and then slightly increased with adding 0.8 wt. % of TiO₂ nanoparticles.

Table 1. Roughness parameters of membrane surface calculated with DME SPM software

membrane	R _a (nm)	RSM(nm)
PVB/TiO ₂ (0%)	31.2	13.3
PVB/TiO ₂ (0.1%)	35.6	24.65
PVB/TiO ₂ (0.5%)	37.2	26.3

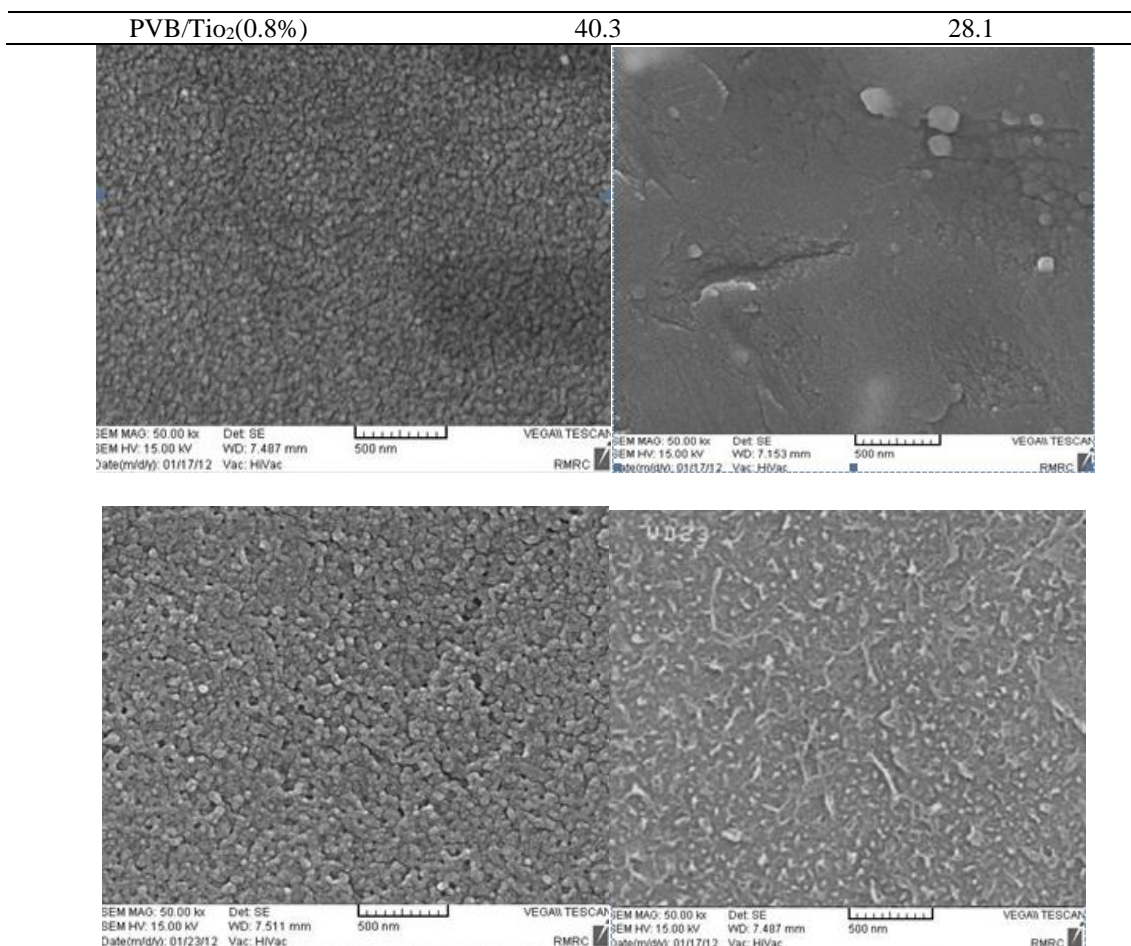


Fig. 4. SEM photographs for PVB/TiO₂ composite polymer membranes: (a) 0 wt.% TiO₂ nanoparticles; (b) 0.1 wt.% TiO₂ nanoparticles; (c) 0.5 wt.% TiO₂ nanoparticles; (d) 0.8 wt.% TiO₂ nanoparticles

Higher hydrophilicity of the modified PVB/ PES membranes in comparison with the unmodified PVB/ PES membrane can be related to hydrophilic nature of TiO₂ nanoparticles and the created hydroxyl groups on the membrane surface due to the presence of TiO₂ nanoparticles. These polar groups can interact with water molecules through van der Waals' force and hydrogen bond. Consequently, the permeation rate of water through the TiO₂ modified PVB/PES composite membranes must be high in comparison with the unmodified one. The accumulation of this nanoparticle at further concentration (more than 0.5 wt.%) on the surface can result an increase on the contact angle of membrane.

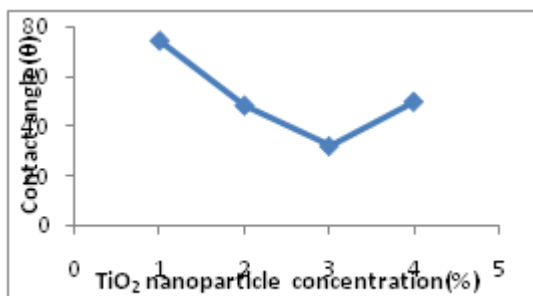


Fig. 5. Contact angle of the prepared membranes.

Pure water flux (PWF)

Fig. 6 reveals the effect of TiO₂ nanoparticles concentration on PWF of the prepared membranes at TMP of 5 bar. As shown, PWF of all modified PES/PVB membranes increased in comparison with that of the virgin PES/PBS membrane. For example, PWF of the membranes increased from 22.1 l/m² h to 55.6 l/m² h after adding 0.5 wt. % of TiO₂ nanoparticles and then slightly decreased with addition of 0.8 wt. % TiO₂ nanoparticles. The above trend confirms the results observed from the aforementioned surface SEM images. In fact, the membranes with higher porosity on top layer presented higher PWF. It is evident that there is a direct relationship between the porosity and permeability at 0.8 wt. % TiO₂ nanoparticles, the flux cannot be improved further as the nano-sized TiO₂ particles coalesce.

Flux and rejection

The effect of TiO₂ concentration on the permeability of the nanofiltration membranes during filtration of yeast wastewater for 90 min is

shown in Fig. 7. The permeability of TiO₂ modified PVB/PES composite membranes are higher than unmodified PVB/ PES membrane. Moreover, the decline in flux of unmodified PVB/PES membrane is highest in comparison with TiO₂modified PVB/PES membranes. The high permeability of TiO₂ modified membranes can be attributed to the high hydrophilicity of membrane surface. The surface of unmodified PVB/PES composite membrane is changed due to the self-assembly of TiO₂ nanoparticles and the surface roughness of TiO₂ modified PVB/PES membrane increased here in (see Table 1). However, the surface hydrophilicity of the membrane also increases with the increase of membrane surface roughness [31].

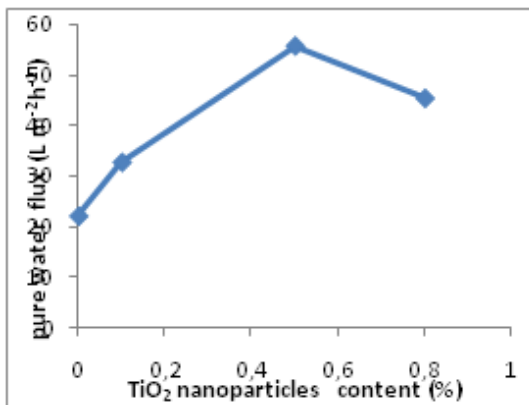


Fig. 6. Effect of TiO₂ nanoparticles concentration on pure water flux

On the other hand, the content of hydroxyl functional group on the membrane surface increases due to the incorporation of TiO₂ nanoparticles into membrane surface. The results of COD rejection of yeast wastewater obtained by utilizing the prepared membranes are illustrated in Fig. 8. As observed, all the modified PES/PVB membranes revealed higher rejection in comparison with the virgin PES/PBS membrane. An increase in TiO₂ nanoparticles concentrations up to 0.5 wt. % resulted in increasing the rejection, however, further increase in TiO₂ nanoparticles concentration up to 0.8 wt. %, resulted in decreasing the COD rejection of the wastewater. Adding TiO₂ nanoparticles in to top layer of membranes change the morphology of membranes and reduce the interaction between hydrophobic particles and membrane's surface. Therefore, in general the rejection is increased.

Swelling measurements

The swelling behavior of membranes was determined in distilled and deionized water. Dry membrane pieces (601 cm² square cut) were placed in distilled and deionized water kept at a constant

temperature, 25°C. The degree of swelling (%) calculated from Eq. (1) for all membranes are plotted as a function of TiO₂ nanoparticles concentration at 25°C (see Fig. 9). PVB uncoated Membrane swell rapidly, and the equilibrium is achieved in about 15 min. It is observed that this membrane has the highest degree of swelling compared to all the other membranes over the studied range of feed water compositions. Swelling degree of the coated membrane decreased from 80 to 38 with increasing TiO₂ nanoparticles concentration. It might be explain that the cross linked PVB/TiO₂ nanocomposite membrane have less accessible free volume for the water and that causes the swelling effect to reduce significantly.

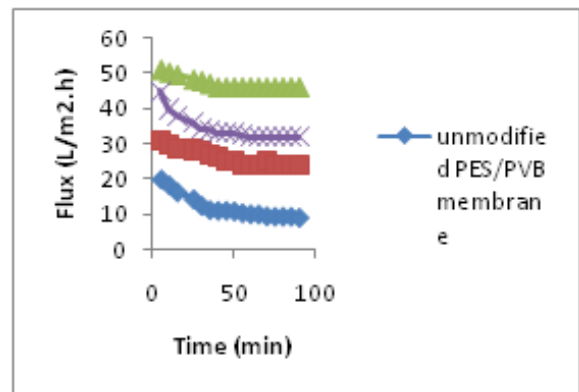


Fig. 7. Permeability of unmodified and modified membranes as a function of TiO₂ content

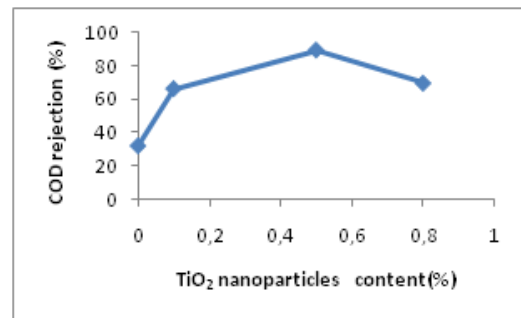


Fig. 8. Effect of TiO₂ nanoparticles content on COD rejection of membranes

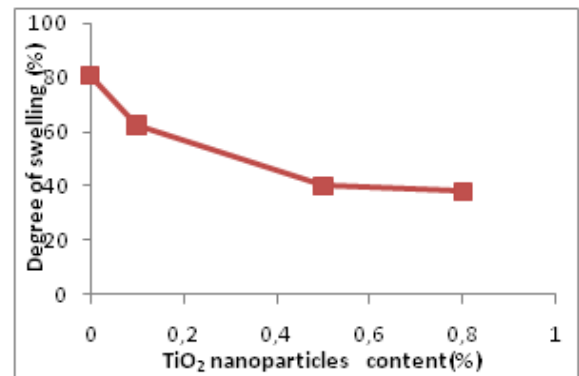


Fig. 9. Degree of swelling of membranes as a function of TiO₂ nanoparticles content.

Binding TiO₂ nanoparticles with PVB hydroxyl groups leads to a compact structural membranes that are in agreement with results obtained from swelling data. Actually, the presence of TiO₂ nanoparticles may improve the roll of cross linking agent and hinder the fact of membrane swelling.

CONCLUSION

In this work, new PVB/PES integral membranes were fabricated and modified by adding TiO₂ nanoparticles on their surfaces to improve the membrane performance and surface properties. The SEM and AFM images confirmed the settling of TiO₂ nanoparticles on the surface of PVB/PES integral membranes. The contact angle measurement indicated that the hydrophilic property of PVB/PES integral membrane was significantly improved by coating of TiO₂ nanoparticles. The water permeability of TiO₂ modified PVB/PES integral membranes were higher than unmodified PVB/PES membrane. Moreover, the flux decline of unmodified PVB/PES membrane was highest. As final result, the COD rejection as a pollution index enhanced considerably from 32 % for unmodified membrane to 89.6% for 0.5% TiO₂ modified membrane which was a superior finding for such membrane performance.

REFERENCES

1. P. Cote, D. Thompson, *Water Sci. Technol.*, **41**, 209 (2000).
2. B. Jefferson, A.L. Laine, S.J. Judd, T. Stephenson, *Water Sci. Technol.*, **41**, 197 (2000).
3. C.N. Lopes, J. Carlos, C. Petrus, H.G. Riella, *Desalination*, **172**, 77 (2005).
4. S. Chakraborty, M.K. Purkait, S. DasGupta, S. De, J.K. Basu, *Sep. Purif. Technol.*, **31**, 141 (2003).
5. M. Mantta ri, K. Viitikko, M. Nystrom, *J. Membr. Sci.*, **272**, 152 (2006).
6. V. Uyak, I. Koyuncu, I. Oktem, M. Cakmakci, I. Toroz, *J. Hazard. Mater.*, **52**, 789 (2008).
7. S. Bouranene, P. Fievet, A. Szymczyk, M. El-Hadi Samar, A. Vidonne, *J. Membr. Sci.*, **325**, 150 (2008).
8. E.M. Vrijenhoek, S. Hong, M. Elimelech, *J. Membr. Sci.*, **188**, 115 (2001).
9. S. Hong, M. Elimelech, *J. Membr. Sci.*, **132**, 159 (1997).
10. Q. Li, M. Elimelech, *Environ. Sci. Technol.*, **38**, 4683 (2004).
11. N. Her, G. Amy, C. Jarusutthirak, *Desalination*, **132**, 143 (2000).
12. S. Bhattacharjee, G.M. Johnston, *Environ. Eng. Sci.*, **19**, 399 (2002).
13. J.G. Choi, T.H. Bae, J.H. Kim, *J. Membr. Sci.*, **203**, 103 (2002).
14. A. Rahimpour, S.S. Madaeni, *J. Membr. Sci.*, **360**, 371 (2010).
15. C. Zhao, J. Xue, F. Ran, S. Sun, *Prog Mater Sci.*, **58**, 76 (2013).
16. A. Ananth, G. Arthanareeswaran, H. Wang, *Desalination*, **287**, 61 (2012).
17. N. Maximous, G. Nakhla, W. Wan, K. Wong, *J. Membr. Sci.*, **341**, 67 (2009).
18. P. Xu, J.E. Drewes, T.U. Kim, C. Bellona, G. Amy, *J. Membr. Sci.*, **279**, 165 (2006).
19. Y.Q. Wang, L.Y. Su, Q. Sun, X.L. Ma, Z.Y. Jiang, *J. Membr. Sci.*, **286**, 228 (2006).
20. N.K. Saha, M. Balakrishnan, M. Ulbricht, *Desalination*, **249**, 1124 (2009).
21. Q. Shi, Y. Su, X. Ning, W. Chen, J. Peng, Z. Jiang, *J. Membr. Sci.*, **347**, 62 (2010).
22. K.R. Kull, M.L. Steen, E.R. Fisher, *J. Membr. Sci.*, **246**, 203 (2005).
23. F. Shen, X. Lu, X. Bian, L. Shi, *J. Membr. Sci.*, **265**, 74 (2005).
24. S.B. Seymour, C.E. Carraher, *Polymer Chemistry—An Introduction*, 2nd Ed., Marcel Dekker, New York, 1988.
25. B. Gebben, H.W.A. van den-Berg, D. Bargeman, C.A. Smolders, *Polymer*, **26**, 1737 (1985).
26. V. Macho, M. Fabini, M. Rusina, S. Bobula, M. Harustiak, *Polymer*, **35**, 5773 (1994).
27. A. Sotto, A. Boromand, R. Zhang, P. Luis, J. M. Arsuaga, J. Kim, B. Van der Bruggen, *J. Colloid Interface Sci.*, **363**, 540 (2011).
28. A. Rahimpour, S.S. Madaeni, A.H. Taheri, Y. Mansourpanah, *J. Membr. Sci.*, **330**, 297 (2009).
29. D. Tanyolac, H. Sonmezis, A.R. Ozdural, *Biochem. Eng. J.*, **22**, 221 (2005).
30. E. Saljoughi, S.M. Mousavi, *Sep. Purif. Technol.*, **90**, 22 (2012).
31. W.Y. Chuang, T.H. Young, W.Y. Chiu, *J. Membr. Sci.*, **172**, 241 (2000).